Chemisorption and Reaction Characteristics of Methyl Radicals on Cu(110)

Run-Sheng Zhai,[†,‡] Yuet Loy Chan,[†] Ping Chuang,[†] Chien-Kui Hsu,[†] Manabendra Mukherjee,[§] Tung J. Chuang,*[,†] and Ruth Klauser[||]

Center for Condensed Matter Sciences, National Taiwan University, Taipei 106, Taiwan, Dalian Institute of Chemical Physics, Chinese Academy of Sciences, Dalian 116023, People's Republic of China, Surface Physics Division, Saha Institute of Nuclear Physics, Calcutta 700064, India, and National Synchrotron Radiation Research Center, Hsinchu 300, Taiwan

Received December 5, 2003. In Final Form: February 18, 2004

Methyl radicals are generated by pyrolysis of azomethane, and the condition for achieving neat adsorption on Cu(110) is described for studying their chemisorption and reaction characteristics. The radical−surface system is examined by X-ray photoemission spectroscopy, ultraviolet photoemission spectroscopy, temperature-programmed desorption, low-energy electron diffraction (LEED), and high-resolution electron energy loss spectroscopy under ultrahigh vacuum conditions. It is observed that a small fraction of impinging CH_3 radicals decompose into methylene possibly on surface defect sites. This type of CH_2 radical has no apparent effect on CH_3(ads) surface chemistry initiated by dehydrogenation to form active CH_2(ads) followed by chain reactions to yield high-mass alkyl products. All thermal desorption products, such as H_2, CH_4, C_2H_4, C_2H_6, and C_3H_6, are detected with a single desorption peak near 475 K. The product yields increase with surface coverage until saturation corresponding to 0.50 monolayer of CH_3(ads). The mass distribution is, however, invariant with initial CH_3(ads) coverage, and all desorbed species exhibit first-order reaction kinetics. LEED measurement reveals a c(2 × 2) adsorbate structure independent of the amount of gaseous exposure. This strongly suggests that the radicals aggregate into close-packed two-dimensional islands at any exposure. The islanding behavior can be correlated with the reaction kinetics and is deemed to be essential for the chain propagation reactions. Some relevant aspects of the CH_3/Cu(111) system are also presented. The new results are compared with those of prior studies employing methyl halides as radical sources. Major differences are found in the product distribution and desorption kinetics, and these are attributed to the influence of surface halogen atoms present in those earlier investigations.

1. Introduction

The chemisorbed methyl radical has been postulated to be an important intermediate in many hydrocarbon surface catalytic processes. They are very difficult to identify under regular high-pressure reaction conditions. Therefore, many recent efforts[1] have been directed to investigate the adsorption and reaction behavior of the radicals on single-crystal metal surfaces in ultrahigh vacuum (UHV) systems in order to understand their basic reaction steps and mechanisms. It is found that on most transition metal surfaces, such as Ni,[2−5] Co,[2] and Fe,[6] there is a great tendency for methyl radicals to dehydrogenate forming carbon and gaseous hydrogen. In contrast, on more noble metal surfaces, such as Cu and Ag, dehydrogenation is suppressed and the likelihood for C−C coupling to yield high-mass species is greatly enhanced. For instance, methyl radicals were shown to be able to couple on Ag(111) below 300 K to produce ethane[7−9] and to react on Cu(111),[10−12] Cu(100),[13] and Cu(110)[14−16] above 300 K to generate long-chain alkyl (C_{2+}) products. Thus, quite a few studies have been undertaken using CH_3(ads)/Cu as a model catalytic system.

In most methyl−metal surface studies to date, methyl halides were employed as a molecular adsorbate. Typically, they were deposited on solid surfaces at low temperatures and decomposed by thermal or photochemical treatments to form the radicals and other products.[10−21] The products were examined by various surface and gaseous analytical tools. The problem associated with this approach is that it is impossible to avoid the influence of coadsorbed halogen atoms on the reaction pathways and kinetics of the radicals. Another means to generate the methyl radicals is by thermal decomposition of azomethane gas initially

* Corresponding author. E-mail: chuangtj@ccms.ntu.edu.tw.
† National Taiwan University.
‡ Dalian Institute of Chemical Physics.
§ Saha Institute of Nuclear Physics.
|| National Synchrotron Radiation Research Center.

(1) Bent, B. E. *Chem. Rev.* **1996**, *96*, 1361 and references therein.
(2) Steinbach, R.; Kiss, J.; Krall, R. *Surf. Sci.* **1985**, *157*, 401.
(3) Zhou, X. L.; White, J. M. *Surf. Sci.* **1988**, *194*, 438.
(4) Zhou, X. L.; White, J. M. *Chem. Phys. Lett.* **1987**, *142*, 376.
(5) Marsh, E. P.; Tabares, F. L.; Schneider, M. R.; Gilton, T. L.; Meier, W.; Cowin, J. P. *J. Chem. Phys.* **1990**, *92*, 2004.
(6) Benziger, J. B.; Madix, R. J. *J. Catal.* **1980**, *65*, 49.
(7) Zhou, X. L.; White, J. M. *Surf. Sci.* **1991**, *241*, 259.
(8) Zhou, X. L.; White, J. M. *Surf. Sci.* **1991**, *241*, 270.
(9) Wu, H. J.; Hsu, H.-K.; Chiang, C. M. *J. Am. Chem. Soc.* **1999**, *121*, 4433.
(10) Lin, J. L.; Bent, B. E. *J. Vac. Sci. Technol.* **1992**, *A10*, 2202.
(11) Lin, J. L.; Bent, B. E. *J. Phys. Chem.* **1993**, *97*, 9713.
(12) Chiang, C. M.; Bent, B. E. *Surf. Sci.* **1992**, *279*, 79.
(13) Lin, J. L.; Chiang, C. M.; Jenks, C. J.; Yang, M. X.; Wentzlaff, T. H.; Bent, B. E. *J. Catal.* **1994**, *147*, 250.
(14) Chiang, C. M.; Wentzlaff, T. H.; Bent, B. E. *J. Phys. Chem.* **1992**, *96*, 1836.
(15) Chiang, C. M.; Wentzlaff, T. H.; Jenks, C. J.; Bent, B. E. *J. Vac. Sci. Technol.* **1992**, *A10*, 2185.
(16) Jenks, C. J.; Bent, B. E.; Zaera, F. *J. Phys. Chem. B* **2000**, *104*, 3017.
(17) Yang, Q. Y.; Maynard, K. J.; Johnson, A. D.; Ceyer, S. T. *J. Chem. Phys.* **1995**, *102*, 7734.
(18) Colaianni, M. L.; Chen, P. J.; Gutleben, H.; Yates, J. T., Jr. *Chem. Phys. Lett.* **1992**, *191*, 561.
(19) Weldon, M. K.; Friend, C. M. *Surf. Sci.* **1994**, *321*, L202.
(20) Bol, C. W. J.; Friend, C. M. *J. Am. Chem. Soc.* **1995**, *117*, 8053.
(21) McBreen, P. H.; Monim, S. S.; Ayyoob, M. *J. Am. Chem. Soc.* **1992**, *114*, 2391.

10.1021/la036294u CCC: $27.50
Published on Web 04/02/2004

developed by Stair and co-workers[22−24] in the form of a nozzle source. The gaseous radicals can be directed onto a solid substrate maintained at a desirable temperature. We and some other groups have also adopted this method.[12,25−31] In this approach, the gaseous species exposed to the substrate are mainly CH_3, N_2, and the parent $CH_3N_2CH_3$ with minor components of CH_4, C_2H_4, and C_2H_6.[27] Depending on the surface structure and chemical nature of the substrate, the effect of residual gases other than the methyl radicals on the surface chemistry has to be taken into account. For instance, all the residual species of N_2, $CH_3N_2CH_3$, and other hydrocarbons have no significant interactions with the Cu(111) surface at 300 K. Therefore, the CH_3(ads)/Cu(111) system with the substrate at 300 K or higher may be investigated free of other surface contaminants. For the CH_3(ads)/Cu(110) system, however, the residual azomethane can strongly interact with Cu(110). We have developed the means to prepare clean CH_3 adsorption on this surface in this report.

In prior studies on Cu surfaces by Bent et al.[1,10−16] with CH_3I as the source for methyl radicals, the production and desorption of CH_4, C_2H_4, and C_3H_6 were detected at 450 K on Cu(111)[10] and at 470 K on Cu(100),[13] all independent of surface coverages following the first-order reaction kinetics, whereas on Cu(110),[14,15] C_2H_4 was the only alkene observed by temperature-programmed desorption (TPD) with the desorption peak at 470 K. On all Cu surfaces investigated by Bent's group, C_2H_6 desorption was found at a slightly lower temperature than those of the alkene products and shown to behave like the second-order kinetics. Namely, C_2H_6 desorption peak temperatures shifted to lower values at higher CH_3(ads) surface coverages. The research group suggested methyl radical dissociation by α-elimination of a hydrogen atom to be the rate-limiting step, followed by reductive elimination of methyl radicals to evolve CH_4 and methylene insertion to produce ethylene and propylene as well as methyl coupling to form ethane. Specifically, the reaction scheme can be represented by $CH_3(ads) \rightarrow CH_2(ads) + H(ads)$ followed by $CH_3(ads) + H(ads) \rightarrow CH_4(g)\uparrow$ and $CH_3(ads) + CH_2(ads) \rightarrow C_2H_5(ads) \rightarrow C_2H_4(g)\uparrow + H(ads)$. Subsequently, the C_3 species can be generated by $C_2H_5(ads) + CH_2(ads) \rightarrow C_3H_7(ads) \rightarrow C_3H_6(g)\uparrow + H(ads)$, and by extension higher mass alkenes can be obtained by $C_3H_7(ads) + CH_2(ads) \rightarrow C_4H_9(ads) \rightarrow C_4H_8(g)\uparrow + H(ads)$, and so forth. In other words, there is a sequential methylene insertion at the α-carbon position into the transient alkyl species to yield longer hydrocarbon chains. In addition, ethane is produced by $CH_3(ads) + CH_3(ads) \rightarrow C_2H_6(g)\uparrow$. This sequential reaction scheme was found to be operative also by Stair et al. on an oxygen-modified Mo surface[32,33] and NiO,[34] with CH_3 generated by azomethane pyrolysis. The kinetic behavior was similar to that of the Cu system. For instance, on oxygen-modified Mo(100), all alkene products up to C_5H_{10} were detected at nearly the same temperature of 440 K. Our recent study on CH_3/Cu(111) also shows that CH_4, C_2H_4, C_3H_6, and C_4H_8 products are evolved at the temperature of 437 K independent of initial CH_3(ads) surface coverage.[29] Clearly, in all these CH_3/surface systems, there are common CH_3(ads) adsorption, reaction, and product desorption characteristics. Yet according to the chemical equations outlined above, the reaction rate for C_2H_4(g) generation should be proportional to both the surface concentrations of methyl and methylene radicals, that is, [CH_3(ads)] and [CH_2(ads)]. Likewise, the C_3H_6(g) yield should depend on [CH_3(ads)] and [CH_2(ads)].[2] Namely, the yields of C_2H_4, C_3H_6, and higher mass alkene products should be proportional to [CH_3(ads)]^n with $n > 1$. Moreover, the TPD peak shapes and temperatures should vary with CH_3(ads) surface concentration. Such TPD characteristics, however, would be in drastic contradiction to the experimental observation. The critical question is why the reaction kinetics leading to the long-chain hydrocarbons can still be first-order regardless of the CH_3(ads) surface coverage, even when the average [CH_3(ads)] concentration is only a small fraction of the saturation coverage. This important issue has not been addressed in the prior studies by the research groups mentioned above or any others.

In the first-order kinetics involving chain reactions, the reactants cannot afford to take time-consuming diffusion steps on the surface. If the reactants were to reside far apart in the adsorption states, there would be little chance to couple within the effective lifetime of the transient species. In other words, lateral interactions of the adsorbates must be considered in trying to understand the reaction kinetics. We have therefore looked into the chemisorption geometry of CH_3(ads) on Cu(111) by low-energy electron diffraction (LEED).[29] It is found that methyl radicals on this relatively smooth surface tend to aggregate to form two-dimensional (2D) islands with $(\sqrt{3} \times \sqrt{3})R30°$ structure even at submonolayer coverages. The proximity of the reactants in the islands is apparently essential in evolving all products from CH_3/Cu(111) at the same temperature and independent of the initial average CH_3(ads) surface concentration. It is then obviously useful to extend the study to the CH_3/Cu(110) system in order to verify the concept, since the (110) face is more corrugated than (111) and may have different chemisorption and reaction behavior. The objective of this report is to present the adsorption and reaction characteristics of methyl radicals on Cu(110) under the cleanest CH_3 exposure condition and to elucidate the reaction kinetics with the chemisorption geometry.

2. Experimental Section

The experiments were carried out in two UHV chambers (base pressure ~ 2×10^{-10} Torr) equipped for X-ray photoemission spectroscopy (XPS), ultraviolet photoemission spectroscopy (UPS), Auger electron spectroscopy (AES), TPD, LEED, and high-resolution electron energy loss spectroscopy (HREELS) as described previously.[25,27,29] Mg Kα (1253.6 eV) and He I (21.2 eV) radiation sources were used for XPS and UPS, respectively. Au($4f_{7/2}$) at 84.0 eV was employed for calibration of binding energies (BEs). To determine the relative yields of hydrocarbon products in the thermal desorption measurement, the mass

(22) Smudde, G. H., Jr.; Viswanathan, R.; Peng, X. D.; Stair, P. C. *J. Vac. Sci. Technol.* **1991**, *A9*, 1885.
(23) Peng, X. D.; Viswanathan, R.; Smudde, G. H., Jr.; Stair, P. C. *Rev. Sci. Instrum.* **1992**, *63*, 3930.
(24) Fairbrother, D. H.; Peng, X. D.; Viswanathan, R.; Stair, P. C.; Trenary, M.; Fan, J. *Surf. Sci.* **1993**, *285*, 2455.
(25) Chan, Y. L.; Chuang, P.; Chuang, T. J. *J. Vac. Sci. Technol.* **1998**, *A16* (3), 1023.
(26) Chan, Y. L.; Chuang, P.; Chuang, T. J.; Klauser, R. *Surf. Sci.* **1998**, *402−404*, 125.
(27) Chuang, T. J.; Chan, Y. L.; Chuang, P.; Klauser, R. *J. Electron Spectrosc. Relat. Phenom.* **1999**, *98−99*, 149.
(28) Chuang, T. J.; Chan, Y. L.; Chuang, P.; Klauser, R.; Ko, C. H.; Wei, D. H. *Appl. Surf. Sci.* **2001**, *169−170*, 1.
(29) Chuang, P.; Chan, Y. L.; Chien, S. H.; Song, K. J.; Klauser, R.; Chuang, T. J. *Langmuir* **2002**, *18*, 4549.
(30) Chuang, P.; Chan, Y. L.; Chien, S. H.; Klauser, R.; Chuang, T. J. *Chem. Phys. Lett.* **2002**, *354*, 179.
(31) Pascal, M.; Lamont, C. L. A.; Kittel, M.; Hoeft, J. T.; Constant, L.; Polcik, M.; Bradshaw, A. M.; Toomes, R. L.; Woodruff, D. P. *Surf. Sci.* **2002**, *512*, 173.
(32) Kim, S. H.; Stair, P. C. *J. Am. Chem. Soc.* **1998**, *120*, 8535.
(33) Kim, S. H.; Stair, P. C. *J. Phys. Chem. B* **2000**, *104*, 3035.
(34) Dickens, K. A.; Stair, P. C. *Langmuir* **1998**, *14*, 1444.

spectrometer (QMS-UTI 100C) was calibrated using methane, ethylene, ethane, and propylene gas standards. Each gas was admitted to the chamber in the pressure range from 10^{-9} to 10^{-7} Torr to obtain the mass spectrum. A very good linearity was found between the intensities of the mass spectrum and the ion gauge reading for each gas. After correction for the different ion gauge sensitivities,[35] the relative ion signals could be normalized to $m/e = 16$ for methane. For instance, the relative QMS sensitivity factors for CH_4 were found to be 1.00, 0.84, and 0.20 at $m/e = 16$, 15, and 14, respectively. Those for C_2H_4 at $m/e = 28$, 27, and 26 were 0.66, 0.42, and 0.44, those for C_3H_6 at $m/e = 42$, 41, 39, and 27 were 0.31, 0.49, 0.40, and 0.25, and so forth. The QMS was differentially pumped with a turbomolecular pump (Balzers TPU 330) and shielded from the chamber with a stainless steel tube and a skimmer of 2 mm diameter aperture. By positioning the Cu(110) crystal surface about 2 mm from the aperture of the skimmer, we could ensure that the molecules detected in TPD were evolved from the sample rather than the sample holder or other parts of the UHV chamber. For most TPD measurements, the sample heating rate was maintained at 3.0 K/s. The HREELS spectrometer (VSW IB2000) had an ultimate spectral resolution of 1 meV full width at half-maximum (fwhm of elastic peak), but for most measurements as presented, a resolution of 3.5 meV was adopted for easier operation. For LEED measurement (VG RV009, beam energy < 70 eV), the charge deposition on the sample was carefully controlled to minimize the electron irradiation effect, and the patterns were recorded with a CCD camera cooled by LN_2.

The Cu(110) sample was initially cleaned by 4−5 h of repeated cycles of ion bombardment (1 kV Ar^+ beam) at 300 K, followed by annealing in UHV (10 min at 970 K) to remove the primary impurities of oxygen, carbon, and sulfur. Surface cleanliness and structure, verified by AES, XPS, UPS, and LEED, were routinely achieved by a single sputtering/annealing cycle. Methyl radicals were generated from azomethane synthesized following the procedure described by Renaud and Leitch[36] through a high-temperature quartz nozzle source.[22,23,25,27] The adsorbate chemisorption characteristics were examined by XPS, UPS, LEED, and HREELS, and the thermal reaction products were determined by TPD.

3. Results and Discussion

3.1. Preparation of Clean Methyl Radical Adsorption on Cu(110). The method to generate methyl radicals via the pyrolysis of azomethane was reported in detail previously.[25,27] When the quartz nozzle source is operated at 1100 K as employed in the present experiment, the radical conversion yield can be as high as 80%.[27] The remaining parent azomethane molecules can still have significant interactions with Cu(110) depending on the substrate temperature. With Cu(110) at 300 K, azomethane readily decomposes, resulting in the adsorption of methylnitrene (NCH_3) on the surface.[37] Therefore, when Cu(110) is exposed to the CH_3 nozzle source, the effect of azomethane has to be taken into account. We have found previously by XPS and HREELS that at low CH_3 exposure, a substantial amount of NCH_x ($x = 2$, 3) is coadsorbed with CH_3(ads) on Cu(110), and the methylnitrene species can be replaced by the incoming methyl radicals at high gaseous exposures.[30,37] With a more sensitive analytical technique, such as TPD, we further observe that quite often a residual quantity of methylnitrene radicals can still be present on Cu(110), when the gaseous exposure is performed at 300 K substrate temperature. Figure 1 depicts the TPD spectra with $m/e = 15$, 43, and 58 for 1.8 langmuir (L) of pure azomethane adsorbed on Cu(110) at 90 K. There are a sharp peak erupted at 130 K and a broad peak centered around 190 K as well as a higher temperature peak located at 375 K. The intensity ratios of these mass signals show all three peaks at 130, 190, and 375 K are due to molecular azomethane because the relative intensities (integrated areas) of these peaks are consistent with the QMS cracking pattern of azomethane. Obviously, there are multilayers of $CH_3N_2CH_3$ adsorbed on the surface at the given gaseous exposure at 90 K. At very small azomethane exposure, we observe only a single desorption peak at 375 K for all three mass signals. As the surface coverage increases, the second TPD peak near 190 K appears followed by the third peak at 130 K. This TPD behavior is somewhat similar to that of azomethane on Pt(111)[38] and Pd(111),[39] and the peaks can be readily assigned to the bulklike multilayer molecules at 130 K, the first-second physisorbed adlayer at 190 K, and the first chemisorbed layer at 375 K. It is further observed that chemisorbed $CH_3N_2CH_3$ decomposes on Cu(110) above 190 K to form methylnitrene which can be desorbed as azomethane molecule by recombination of the radical species around 375 K. Because of this complication due to the presence of azomethane in the CH_3 radical source, we decide to carry out the gaseous exposure with Cu(110) at 400 K substrate temperature. Figure 2 illustrates the difference of TPD spectra for CH_4 (with $m/e = 14$ and 15) between the CH_3 exposure with Cu(110) at 300 K and that at 400 K. The additional peak at 384 K associated with the surface maintained at 300 K during CH_3 exposure is apparently due to the effect of residual azomethane in the radical source. With Cu(110) held at 400 K during the

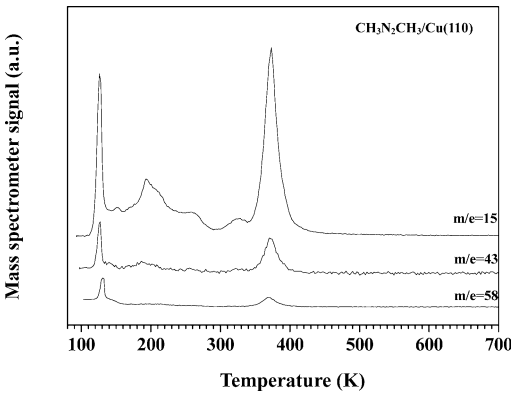

Figure 1. TPD spectra monitoring $m/e = 15$, 43, and 58 with a multilayer of azomethane on Cu(110) at 90 K.

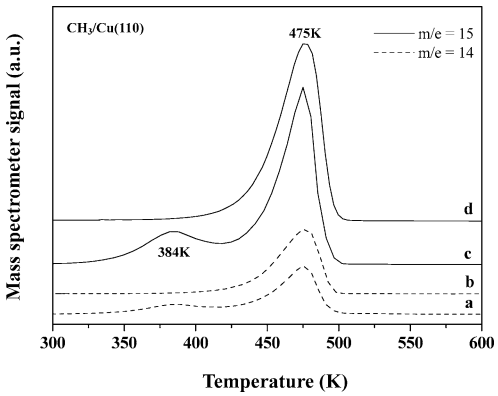

Figure 2. TPD spectra monitoring $m/e = 15$ and $m/e = 14$ from saturated coverage of CH_3(ads) on Cu(110) with the substrate temperature at 300 K (a,c) and 400 K (b,d), respectively.

(35) *NASA Technical Note TND-5285*; National Aeronautics and Space Administration: Washington, DC, June, 1969.
(36) Renaud, R.; Leitch, L. C. *Can. J. Chem.* **1954**, *32*, 545.
(37) Chuang, P.; Chan, Y. L.; Chuang, C. H.; Chien, S. H.; Chuang, T. J. *Appl. Surf. Sci.* **2001**, *169−170*, 153.
(38) Jentz, D.; Trenary, M.; Peng, X. D.; Stair, P. C. *Surf. Sci.* **1995**, *341*, 282.
(39) Hanley, L.; Guo, X.; Yates, J. T., Jr. *Surf. Sci.* **1990**, *232*, 129.

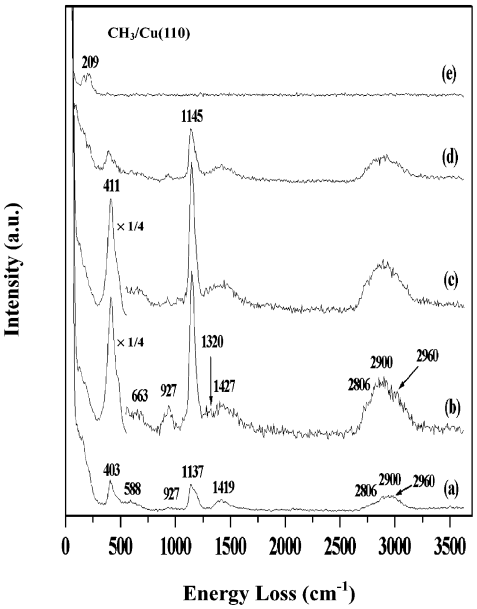

Figure 3. HREELS spectra for saturated methyl radicals on Cu(110) at 400 K (b) and annealing to 460 K (c), 500 K (d), and 530 K (e). The reference spectrum in curve (a) is from a submonolayer coverage of CH_3I on Cu(110) adsorbed at 90 K and annealed to 230 K to form CH_3(ads).

gaseous exposure, clean CH_3(ads) adsorption is achieved and this is the methyl radical deposition condition we have undertaken throughout the present study.

3.2. Chemisorption Characteristics of CH_3(ads) on Cu(110). XPS measurements of CH_3(ads) at the saturated coverage on Cu(110) at 400 K show the C(1s) main peak at 283.2 eV and a shoulder band around 284.6 eV. The integrated intensity ratio of these two components is about 0.85:0.15, similar to the observation of CH_3(ads) on Cu(111).[27] The C(1s) peak at 283.2 eV is assigned to CH_3(ads), and the minor one at 284.6 eV is due to CH_2(ads). The methylene species is most likely from partial dehydrogenation of CH_3(ads) on surface defect sites. Apart from hydrocarbon and copper signals, there is no trace of nitrogen or any other species on the surface in the XPS spectra. As mentioned earlier, CH_3(ads) radicals can be produced also from thermal dissociation of CH_3I on Cu(110).[14,15] Figure 3a displays the HREELS spectrum of a submonolayer coverage of CH_3I which is deposited on Cu(110) at 90 K followed by annealing at 230 K. Such thermal treatment can yield CH_3(ads) and I(ads), and this HREELS spectrum may be utilized as a reference for CH_3(ads), although undoubtedly the vibrational frequencies of the radicals are influenced by the coadsorbed iodine atoms. The HREELS spectrum for saturated CH_3(ads) generated by azomethane pyrolysis following the procedure described in section 3.1 is depicted in Figure 3b. The major peaks appear at 411 cm^{-1} [υ(M−CH_3)], 927 cm^{-1} [$\rho(CH_3)$], 1145 cm^{-1} [$\delta_s(CH_3)$], 1427 cm^{-1} [$\delta_{as}(CH_3)$], 2806 cm^{-1} [$2\delta_{as}(CH_3)$, F.R.], 2900 cm^{-1} [$\upsilon_s(CH_3)$], and 2960 cm^{-1} [$\upsilon_{as}(CH_3)$], all clearly due to chemisorbed CH_3(ads) radicals. The minor signals near 663 and 1320 cm^{-1} may be associated with the small amount of CH_2(ads) which should exhibit other characteristic vibrational modes. The frequencies of those modes are, however, rather close to CH_3(ads) bands and difficult to distinguish under the present condition, for example, $\omega(CH_2)$ near 1145 cm^{-1} and $\upsilon(CH_2)$ near 2960 cm^{-1}. The observed vibrational frequencies and band assignments for CH_3(ads) on both Cu(110) and Cu(111) are consistent with those of prior studies as listed in Table 1. When the surface temperature is raised, the intensities

Table 1. Observed Vibrational Frequencies (cm^{-1}) and Mode Assignments for CH_3/Cu(110) and CH_3/Cu(111)

(cm^{-1})	CH_3/Cu(110) (present work)	CH_3/Cu(110) from CH_3I dissociation (present work)	CH_3/Cu(111) (ref 27)	CH_3/Cu(111) (ref 12)
411	ν(M−CH_3)	403	371	355
	ν(M−C)	588	532	
663	ν(M−CH_2)		645	
927	$\rho_r(CH_3)$	927	734	890
1145	$\delta_s(CH_3)$, $\omega(CH_2)$	1137	1169	1190
1320	$\delta(CH_2)$		1371	1380
1427	$\delta_{as}(CH_3)$	1419	1371	
2806	$2\delta_{as}(CH_3)$ F.R.	2806	2710	
2900	$\nu_s(CH_3)$	2900	2790	2790
2960	$\nu_{as}(CH_3)$, $\nu(CH_2)$	2960	2940	2945

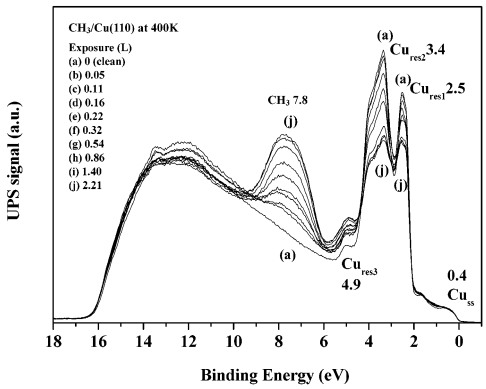

Figure 4. UPS spectra taken during adsorption of methyl radicals on Cu(110) at 400 K.

of all vibrational bands attributed to CH_x gradually decrease without the appearance of any new feature (Figure 3c,d). As the temperature reaches 530 K, all the peaks essentially disappear, except for a band centered at 209 cm^{-1}. This peak can be assigned to the surface phonon of Cu(110). The disappearance of all peaks indicates that no hydrocarbon species remain on Cu(110) above 530 K. No new vibrational peak is observed in the thermal annealing process. This means that apart from thermal desorption via $CH_3(ads) + H(ads) \rightarrow CH_4(g)\uparrow$, CH_3 dissociation is the rate-limiting step in the surface reactions as suggested originally by Bent's group.[1] Consequently, the reaction intermediates cannot be observed in HREELS spectra. The small quantity of CH_2(ads) present in the initial CH_3(ads) exposure, which is attributed to CH_3(ads) dehydrogenation on surface defect sites mentioned above, seems to persist up to 500 K (Figure 3c,d). This type of CH_2(ads) apparently has no significant interaction with the coadsorbed CH_3(ads) radicals.

Figure 4 shows the UPS spectra taken as a function of CH_3 exposure on a clean Cu(110) surface at 400 K. The clean Cu(110) surface exhibits a surface state (Cu_{ss}) at 0.4 eV BE, which is attributed to the emission from the s−p band of copper, and three surface resonances at 2.5 (Cu_{res1}), 3.4 (Cu_{res2}), and 4.9 eV (Cu_{res3}) due to the emission from the Cu 3d band in agreement with those reported previously.[40,41] Obviously, the signal intensities of the Cu surface state and resonances decrease when the CH_3 exposure and the adsorbate coverage are increased. To see the clear effect of CH_3 adsorption, we take the difference spectra between the CH_3-exposed sample and the clean Cu surface. The results are displayed in Figure

(40) Onsgaard, J.; Quist, S.; Christensen, S. V.; Godowski, P. J.; Nerlov, J. *Surf. Sci.* **1997**, *370*, L137.
(41) Christensen, S. V.; Nerlov, J.; Godowski, P. J.; Onsgaard, J. *J. Chem. Phys.* **1996**, *104*, 9613.

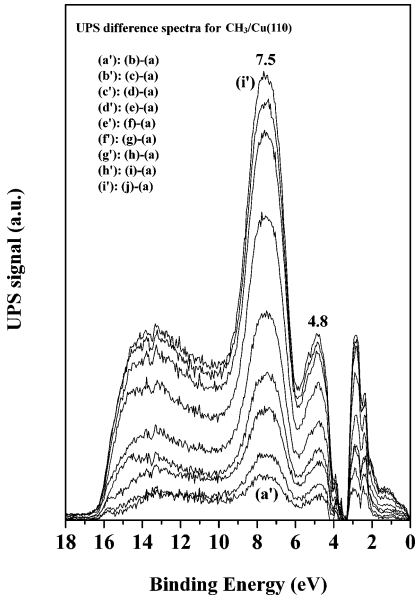

Figure 5. UPS difference spectra displayed in Figure 4 to show the adsorbate valence bands as a function of CH_3 exposure.

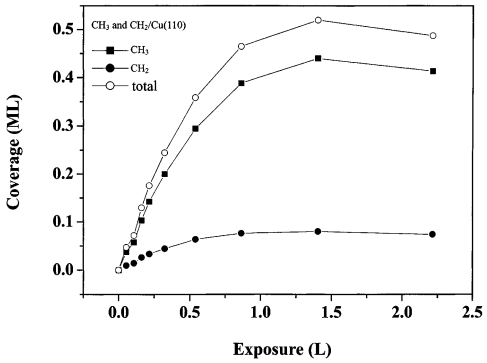

Figure 6. Surface coverages of methyl and methylene radicals on Cu(110) at 400 K as a function of CH_3 exposure until saturation coverage of 0.50 ML.

5. On adsorption, two peaks apparently grow at 7.5 and 4.8 eV BE. The peak at 7.5 eV is assigned to CH_3(ads) according to prior UPS study of iodomethane on Pd(100),[42] which showed one photoemission peak at 8.5 eV attributed to the 1e orbital of the pyramidal CH_3(ads) formed in the dissociation of CH_3I. The peak at 4.8 eV is assigned to CH_2(ads) according to the UPS measurement of diiodomethane on Cu(100),[43] which detected the appearance of a new peak at 5.4−5.6 eV due to CH_2 species from the dissociation of CH_2I_2. From the relative intensities of these two peaks, we can calculate the relative concentrations of the two radical species on Cu(110) as a function of CH_3 exposure, as depicted in Figure 6. In the intensity measurement, we have integrated the peak areas between the valleys. It is clear from Figure 6 that at the saturated CH_3 exposure with the surface at 400 K, there are about 85% of CH_3(ads) and 15% of CH_2(ads) radicals in the surface coverage under the present gaseous exposure condition. This result is practically the same as that determined by XPS.

The UPS spectra as presented for methyl radicals with a small amount of methylene on Cu(110) represent those obtained under the cleanest adsorption condition. In particular, these spectra are acquired free of the influence

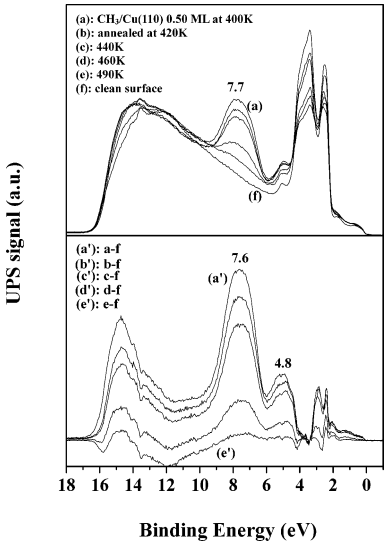

Figure 7. UPS spectra for 0.50 ML CH_3/Cu(110) at 400 K and then annealed to various temperatures as indicated.

and interference of iodine or other halogen atoms often encountered in prior studies. From UPS, we can also determine the work function change ($\Delta\varphi$) of CH_3(ads) on Cu(110), which turns out to be slightly negative, that is, about −0.01 eV. This value is much less than those of adsorbed methane (−1.11 eV), ethane (−1.53 eV), propane (−1.55 eV), ethene (−1.68 eV), and propene (−1.69 eV) on Pt ribbon at 10^{-4}−10^{-2} mbar.[44] This implies there is very little charge transfer from CH_3 to Cu and the adsorbate−substrate interaction is rather weak. Figure 7 depicts the UPS spectra of a CH_3-exposed surface at 400 K with saturated coverage and then annealed to various temperatures. With increasing temperature, the signals attributed to CH_3(ads) and CH_2(ads) drop in intensity and disappear above 530 K. The rate of CH_3(ads) decrease as a function of T in the temperature range of 440−490 K seems to be faster than that of CH_2(ads). For instance, the amount of CH_3(ads) drops by 75% at 460 K and 93% at 490 K, whereas the corresponding decreases for CH_2(ads) are 68% and 83%, respectively. It is known that ordinary CH_2(ads) species can react with CH_3(ads) on Cu(110) below 350 K.[14,30] Since the CH_3/Cu(110) system is prepared at 400 K substrate temperature in the present study, we can be certain that the residual CH_2(ads) at defect sites from the initial CH_3 exposure has no direct effect on the CH_3-(ads) surface chemistry initiated by the dehydrogenation process above 400 K. The UPS result is also consistent with that obtained by HREELS showing once again that the radical adsorbates essentially diminish due to reaction and desorption below 530 K.

The LEED patterns of a clean Cu(110)-(1 × 1) surface and a CH_3(ads)-covered surface at 0.50 monolayer are illustrated in Figure 8. The energies of the electron beam for LEED measurements are fixed at 38 eV (labeled as a) and 67 eV (labeled as b), respectively. At the high e-beam energy, many electron diffraction spots from substrate Cu atoms can be displayed in the given view screen (Figure 8b). For detecting the diffraction spots due to the radical adsorption, a lower e-beam energy is better for viewing the adsorbate patterns. From the LEED patterns as displayed in images a2 and b2 of Figure 8, it is clear that CH_3 radicals are adsorbed with c(2 × 2) structure. According to the atomic density (1.08×10^{15} atoms/cm^2) and the surface structure (2.56 Å × 3.62 Å rectangle unit

(42) Solymosi, F. *Catal. Today* **1996**, *28*, 193.
(43) Kovács, I.; Solymosi, F. *J. Phys. Chem. B* **1997**, *101*, 5397.
(44) Hlavathy, Z.; Tétényi, P. *Surf. Sci.* **1998**, *410*, 39.

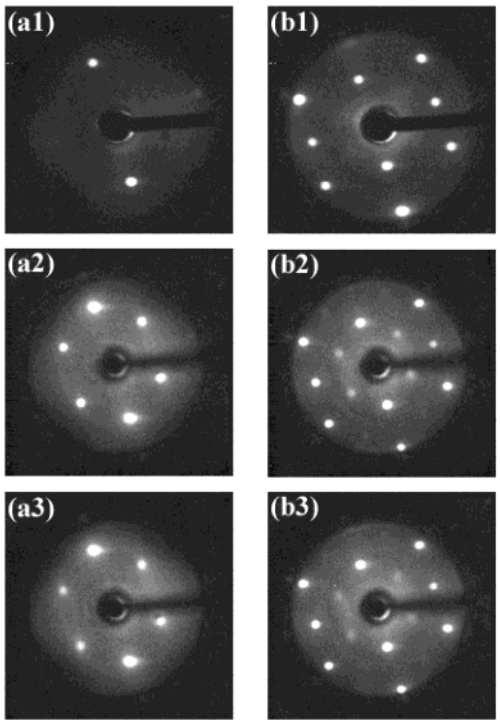

Figure 8. LEED patterns of a clean Cu(110) surface at beam energy 38 eV (a1) and 67 eV (b1), respectively, and 0.50 ML of CH_3(ads) with c(2 × 2) structure (a2,b2) as well as the sample annealed to 450 K (a3,b3).

cell) of Cu(110), the c(2 × 2) pattern indicates that the distance between two nearest methyl radicals is 4.43 Å. From the c(2 × 2) structure for CH_3(ads), we can determine the saturated coverage of methyl radicals to be 0.50 monolayer (ML) (Θ_{ad} in ML, referred to the density ratio between adsorbate molecules and the top surface Cu atoms). This value is clearly much higher than 0.045 which was estimated to be the saturation coverage of CH_3 produced by CH_3I dissociation on Cu(110) in a prior study.[13] The observed c(2 × 2) pattern persists even when the average surface coverage is much less than the saturation coverage. For instance, when the sample at $\Theta_{ad} = 0.50$ ML is briefly annealed to 460 K to reduce the amount of CH_3(ads), the LEED intensity decreases, but the c(2 × 2) structure remains unchanged, as depicted in images a3 and b3 of Figure 8 with Θ_{ad} at around 0.3 ML. The diffraction pattern can still be detected with Θ_{ad} less than 0.15 ML. We surmise that the CH_3 radicals may reside in the open trenches of the Cu(110) surface on the 4-fold hollow sites for maximum coordination of C atoms with neighboring Cu atoms. This consideration is compatible with the finding for CH_3 on Cu(111) in which the radicals clearly prefer to occupy the 3-fold-coordinated hollow sites.[31] A possible chemisorption geometry of CH_3(ads) radicals on the (110) surface is illustrated in Figure 9, showing both the top and side views of surface structure. From the radii of C (r_C) and H (r_H) atoms and the H−C−H angle (θ_{HCH}) in the CH_3(ads) radical, we can calculate the diameter of the methyl radicals to be $2(r_C + 2r_H)\cos(\theta_{HCH} - 90°)$. Given the radii of Cu, C, and H atoms[45] at 1.28, 0.715, and 0.37 Å, respectively, and $\theta_{HCH} = 106°$,[46] we can readily show that the diameter of the methyl radical is about 2.8 Å and the C end of the radical can be in direct contact with the second layer of Cu atoms, as displayed in Figure 9. It is also clear that the c(2 × 2) adsorption

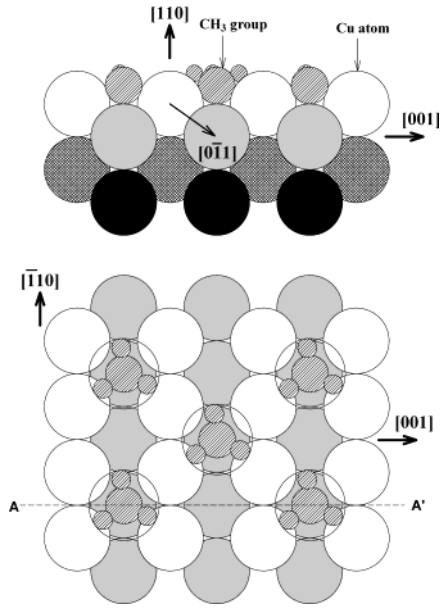

Figure 9. A possible adsorption geometry for the c(2 × 2) structure of CH_3(ads) on Cu(110): top view (bottom part) and side view (top part) along the AA′ line of the top view. CH_3 radicals are represented by circles with oblique lines therein.

geometry is the most compact structure in which the CH_3 radical can freely rotate along the C−Cu axis. The fact that c(2 × 2) structure can still be maintained even with an average surface coverage of 0.15 ML or less indicates the aggregation of CH_3(ads) radicals into the close-packed patterns leaving many patches of the Cu surface unoccupied. This can be visualized in the form of 2D CH_3(ads) islands. In our previous study, we have observed an islanding behavior for methyl radicals adsorbed on Cu(111) exhibiting a $(\sqrt{3} \times \sqrt{3})$R30° LEED pattern from a very small surface coverage to a saturated coverage. This $(\sqrt{3} \times \sqrt{3})$R30° structure has also been detected by Pascal et al.[31] with the photoelectron diffraction method on the same system at both CH_3 saturation and half saturation coverages. Such a pattern is the most close-packed adsorbate structure on Cu(111). In a further study of CH_3(ads) on Cu(111) by scanning tunneling microscopy (STM), we have directly observed the radical aggregation and 2D islanding behavior on the surface. Like the CH_3/Cu(111) system, the 2D island formation has a critical effect on the reaction kinetics of CH_3(ads) on Cu(110).

3.3. Surface Reaction of CH_3(ads) on Cu(110). In TPD analysis, we have tried to monitor all possible hydrocarbon products when the temperature of the CH_3-exposed surface is raised from 300 to 700 K at 3 K/s heating rate. In the mass range from 2 to 90 amu, we observe desorption signals from H_2, CH_4, C_2H_4, C_2H_6, and C_3H_6 species with *m*/*e* at 2, 14, 15, 16, 27, 28, 29, 30, 38, 39, 40, 41, and 42. Some typical multiplexed thermal desorption spectra of 2, 16, 27, 30, and 41 amu signals are illustrated in Figure 10 as a function of CH_3 exposures. From quantitative analysis, it is found that the relative intensity ratios of the 14, 15, and 16 amu desorption signals are about 0.2:0.8:1.0, which are consistent with the cracking pattern for CH_4. Likewise, the desorption signals at 29 and 30 amu can be attributed solely to C_2H_6, but the signals at 26, 27, and 28 amu have contributions from both C_2H_6 and C_2H_4. The signals from 39 to 42 amu are due entirely to desorbed C_3H_6. Accordingly, we can conclude that the primary desorbing species in our TPD measurement are H_2, CH_4, C_2H_4, C_2H_6, and C_3H_6. The relative yields of these products as a function of CH_3 exposure are illustrated in

(45) http://www.webelements.com.
(46) Robinson, J.; Woodruff, D. P. *Surf. Sci.* **2002**, *498*, 203.

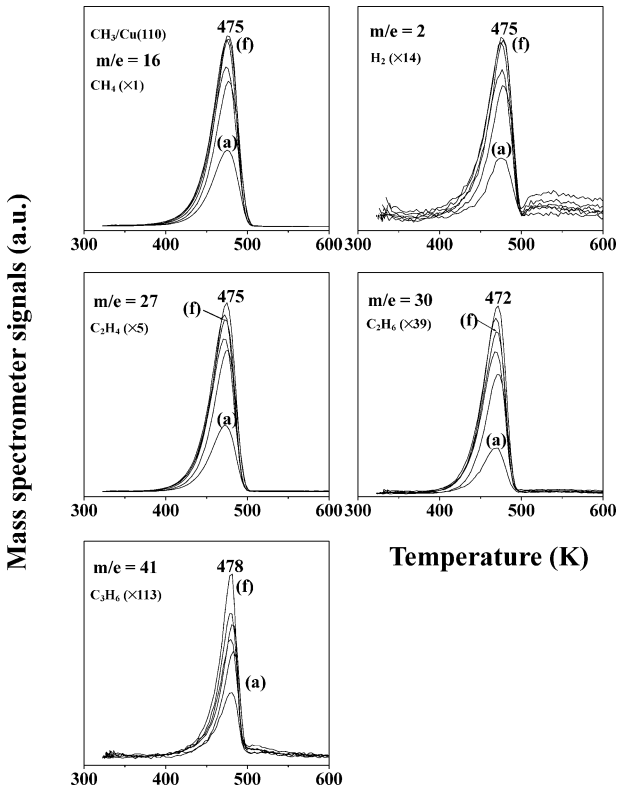

Figure 10. TPD spectra of CH_3/Cu(110) monitoring m/e = 16 (CH_4), 27 (C_2H_4), 41 (C_3H_6), 2 (H_2), and 30 (C_2H_6) as a function of CH_3 exposure: (a) 0.33 langmuir, (b) 0.77 langmuir, (c) 1.70 langmuir, (d) 2.81 langmuir, (e) 4.62 langmuir, and (f) 6.83 langmuir.

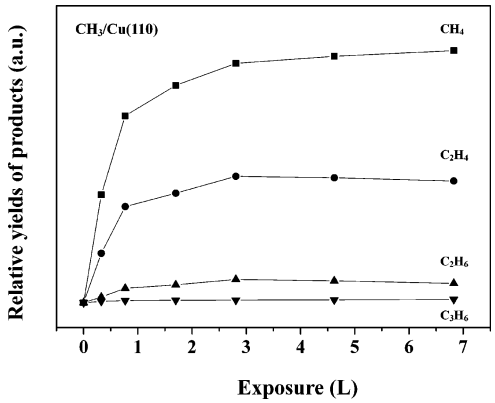

Figure 11. Relative TPD yields of CH_4, C_2H_4, C_2H_6, and C_3H_6 desorbed from Cu(110) as a function of CH_3 exposure.

Figure 11. All the desorbed species are detected with a single TPD peak with the signal maximum at 475(±3) K, independent of CH_3 exposure. In other words, the reaction and desorption processes follow the first-order kinetics for all gaseous products. Using the Redhead desorption equation[47] with the pre-exponential factor of 1×10^{13}/s, we obtain the activation energy to be 29.4(±0.2) kcal/mol.

There are clearly a number of differences between the present result and the TPD data presented by Chiang et al.[14,15] in the study of CH_3/Cu(110) with CH_3I as the methyl source. The major differences appear in the product distributions as well as in the TPD peak shapes and temperatures as a function of gaseous exposure. In the prior work, the detected gaseous products were CH_4, C_2H_4, and C_2H_6, but no H_2 or higher mass hydrocarbons. CH_4 exhibited two TPD peaks with the major one at 470 K which was independent of CH_3I exposure and the minor one shifting from 362 to 325 K with increasing adsorbate coverage. C_2H_6 was observed only at high exposures and displayed a broad band with the peak position moving from 450 to 400 K as exposure was increased. The formation of C_2H_6 was inferred to follow the second-order reaction kinetics. Both the yields of CH_4 and C_2H_4 would reach maximum values and then decline as a function of CH_3I exposure. Such results are in drastic contrast to the present observation which shows that all reaction products obey the first-order kinetics with constant desorption peak temperature, and there are monotonic increases of reaction yields with CH_3 exposure until saturation around 3 langmuir (Figure 11). Furthermore, the relative yields of CH_4, C_2H_4, C_2H_6, and C_3H_6 remain essentially unchanged at about 1:0.5:0.09:0.01 with CH_3 exposure between 0.3 and 3 langmuir. In other words, these relative yields are not affected by the initial CH_3(ads) coverage up to the saturation coverage. We believe the major differences between the two studies are due to the influence of iodine atoms which were present on Cu(110) in the prior work.

The first-order reaction kinetics, the monotonic increase of product yields with CH_3 exposure, and the fact that the product distribution is independent of initial CH_3(ads) coverage strongly suggest the minimal role played by surface diffusion of reagents. Indeed, such reaction characteristics can be correlated very well with the chemisorption geometry of CH_3(ads) radicals. As we have observed by LEED, CH_3(ads) molecules tend to aggregate into c(2 × 2) close-packed structure even at a very small average surface coverage ($\Theta_{ad} \ll 0.5$ ML). As discussed above, the most reasonable interpretation of the LEED data is the formation of 2D islands for the adsorbate and the increase of island sizes with gaseous exposure. Consequently, the surface chemistry of the radicals is dominated by the close-packed molecules inside the islands regardless of the island sizes. In such adsorption geometry, once the active CH_2(ads) molecules are created by CH_3-(ads) dehydrogenation, they can readily react with neighboring CH_3(ads) and other freshly generated CH_2(ads) to start the chain reactions in the production of C_2H_5(ads), C_3H_7(ads), and C_4H_9(ads), which partially desorbed as C_2H_4(g), C_3H_6(g), and C_4H_8(g). The proximity of reagents in the close-packed structure can facilitate the first-order kinetics without the time-consuming diffusion steps which would be necessary if the adsorbates were separated far apart. The first-order kinetic behavior also rules out the possibility of radical chain reactions taking place around the perimeters of the islands. Such reactions would result in fractional orders with desorption peak temperatures strongly dependent on the surface coverages. In this picture of 2D islanding, the product mass distribution should be independent of the island size, but the total product yields should be proportional to the initial average CH_3(ads) coverage. These are in fact observed in the present experiment. We therefore conclude that the 2D-islanding effect is critical for the long-chain hydrocarbon propagation reactions. From this point of view, we can also easily understand the different results between the present study and the prior work. Obviously, surface contaminants such as iodine atoms can strongly affect CH_3(ads) adsorption geometry and interfere with its island formation. This effect is particularly severe at high CH_3I exposures resulting in high iodine concentration on the surface. Since the carbon chain growth is a competing process with desorption, the contaminant can readily interfere to prevent the formation of C_3H_6 or higher mass species. The 2D-islanding phenomenon is also consistent

(47) Redhead, P. A. *Vacuum* **1962**, *12*, 203.

with the first-order kinetics for CH_3(ads) coupling to form C_2H_6(g), in contradiction to the second-order behavior reported by Chiang et al.[14]

3.4. Comparison of CH_3(ads) on Cu(110) and Cu(111). Among the various facets of a Cu crystal, the Cu(111) surface has the highest density of Cu atoms in the surface plane (1.76×10^{15} atoms/cm^2) and the smoothest structure. In contrast, Cu(110) is highly corrugated in one dimension on an atomic scale with rows and troughs. Thus, some differences in chemisorption characteristics and certain common reaction behavior can be expected. When Cu(111) is exposed to azomethane at 300 K, no molecular adsorption or reaction can take place, whereas on Cu(110), the molecule readily decomposes to form NCH_3(ads) on the surface. Therefore, CH_3(ads) adsorption on Cu(111) through the quartz nozzle source does not have significant interference from the undecomposed azomethane gas. As mentioned in section 3.2, both the XPS C(1s) peaks of saturated CH_3/Cu(110) at 400 K and saturated CH_3/Cu(111) at 300 K[27] exhibit two components with the major one at lower BE due to CH_3(ads) and the minor one at higher BE attributed to CH_2(ads). UPS spectra of CH_3/Cu(111) also confirm this interpretation. The vibrational frequencies of the adspecies on both Cu surfaces as listed in Table 1 are actually quite similar. The surface structures of CH_3(ads) on Cu(110) and Cu(111) as obtained by LEED patterns are c(2 × 2) and ($\sqrt{3} \times \sqrt{3}$)R30°, respectively. The distance between two nearest radicals is 4.4 Å for both structures. In both cases, these structures are independent of average CH_3(ads) surface coverage. Recently the 2D-islanding phenomenon for CH_3(ads)/Cu(111) has been directly observed by the STM technique.[48] It is confirmed that the size and shape of the 2D islands can vary depending on the gaseous exposure, but within any given island, CH_3(ads) radicals aggregate to form close-packed ($\sqrt{3} \times \sqrt{3}$)R30° structure even at a very small average surface coverage ($\Theta_{ad} \ll 0.5$ ML). This tendency of CH_3(ads) in forming close-packed 2D patterns due to strong lateral interactions is clearly quite similar on both (110) and (111) surfaces. As discussed above, this adsorption geometry is a crucial factor in promoting the chain growth once the reaction is initiated by the dehydrogenation of CH_3(ads) radicals within an island.

In TPD, we observe that CH_4, C_2H_4, C_3H_6, C_4H_8, and C_5H_{10} are generated with the same peak temperature of 437 K for CH_3(ads)/Cu(111). Some of the TPD spectra as a function of CH_3 exposure are displayed in Figure 12. These alkene products are created with the characteristics of first-order reaction kinetics similar to the CH_3/Cu(110) system. The lower peak desorption temperature implies a lower activation energy (27.2 kcal/mol) on the Cu(111) surface. In the initial report,[29] we thought the formation of C_2H_6 from CH_3(ads) coupling reaction might follow a second-order reaction kinetics. Yet by further measurements, it is determined to be more like the first-order kinetics as well (C_2H_6 TPD spectra also displayed in Figure 12), although the peak desorption temperature is somewhat lower than that of the alkene products. In any case, on Cu(111), C_2H_6 is really a very minor product in comparison with the high-mass alkene yields. The differences in the reaction yields between the (110) and the (111) surfaces may be due to the different mobilities of radical adsorbates and/or the different reactivities of the surface structures with (110) clearly more open than (111). As for the product yields as a function of CH_3 exposure, the TPD signals for all masses increase with the gaseous exposure until saturation above 3 langmuir on Cu(111). This is again in drastic contrast to the CH_3I/Cu(111) system investigated by Lin and Bent,[10,11] in which the yields of CH_4, C_2H_4, and C_3H_6 reached a maximum at 2 langmuir exposure of CH_3I and then declined at higher exposures. The C_2H_6 yield showed an onset at 1 langmuir and increased linearly with the exposure. Furthermore, no alkene longer than C_3H_6 was detected in that prior study. Like the CH_3I/Cu(110) system, the presence of I atoms on the Cu(111) clearly has a profound effect on the CH_3(ads) surface chemistry.

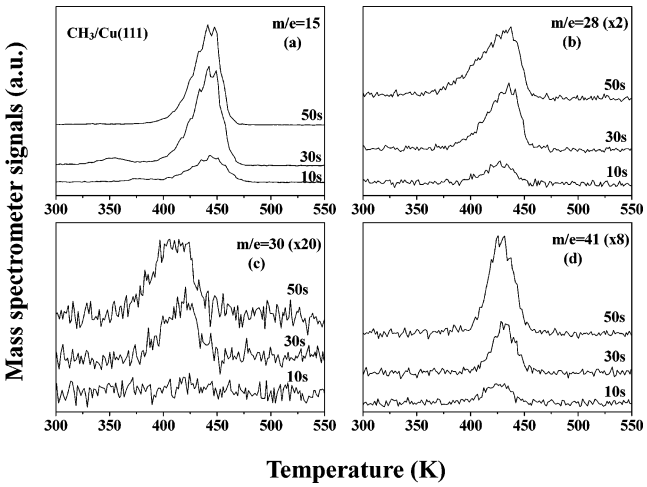

Figure 12. TPD spectra of CH_3/Cu(111) monitoring $m/e = 15$ (CH_4), 28 (C_2H_4), 30 (C_2H_6), and 41 (C_3H_6) as a function of CH_3 exposure time.

4. Conclusions

In this study, we have developed the cleanest method so far to deposit methyl radicals on Cu(110) by means of azomethane pyrolysis. Under the given conditions, a small fraction of the impinging CH_3 radicals decompose into methylene adsorbed possibly on the surface defect sites. The chemisorption characteristics of these adsorbates are analyzed by XPS, UPS, HREELS, and LEED, and the thermal reaction behavior is determined by TPD. The presence of CH_2(ads) in the initial gaseous exposure is confirmed by XPS, UPS, and HREELS spectra, but this type of CH_2(ads) radical is found to have no direct effect on the CH_3(ads) surface chemistry. The thermal reactions of CH_3(ads) are initiated by the dehydrogenation to form active CH_2(ads) followed by sequential chain reactions to yield high-mass alkyl products which are desorbed as C_2H_4 and C_3H_6, in addition to H_2, CH_4, and C_2H_6. All the thermal desorption products generated by CH_3(ads) radicals are detected with a single TPD peak near 475 K, independent of initial CH_3(ads) surface coverage and exhibiting first-order reaction kinetics. The product yields for all species increase monotonically with CH_3 exposure until saturation coverage. The mass distribution of the gaseous products is, however, unaffected by the CH_3(ads) coverage. LEED measurement reveals a c(2 × 2) adsorbate structure which is invariant with the average surface coverage ranging from 0.15 ML to the saturated coverage at 0.50 ML. The result strongly suggests that CH_3(ads) radicals tend to aggregate into close-packed patterns forming 2D islands similar to the CH_3/Cu(111) system, in which the islanding behavior has been directly observed by STM. The close-packed adsorption geometry obviously has a strong impact on the chain reaction kinetics. Namely, the proximity of reagents inside the islands even at a very small surface coverage can render extensive surface diffusion unneces-

(48) Chan, Y. L.; Pai, W. W.; Chuang, T. J. *J. Phys. Chem. B* **2004**, *108*, 815.

sary and readily facilitate the first-order kinetics as detected by TPD. This is true for both CH_3/Cu(110) and CH_3/Cu(111). On Cu(111), alkenes as high as C_5H_{10} can be obtained in the desorption products, whereas C_2H_6 yield due to CH_3 coupling is relatively low. Apparently, the chain reactions of methyl and methylene radicals can be enhanced on the smoother Cu(111) surface as compared to Cu(110). The present results are also compared with those of prior investigations with CH_3I to yield CH_3(ads) radicals on Cu surfaces. Major differences are found in the product distributions and reaction kinetics as a function of gaseous exposure. We attribute the differences to the influence of halogen atoms which are present on the Cu surfaces once methyl halide is used as the adsorbate. Hence, we believe this study represents so far the most reliable determination of CH_3 adsorption and reaction behavior on the Cu(110) surface. The methyl radical 2D-islanding phenomenon may have wider implications in hydrocarbon surface catalysis.

Acknowledgment. The authors thank the National Science Council and the Ministry of Education of R.O.C. for support of this study. One of us (T.J.C.) also thanks Dr. Hans Confal and his colleagues at IBM Almaden Research Center for the kind hospitality and useful discussion during the visiting periods when this paper was prepared.

LA036294U